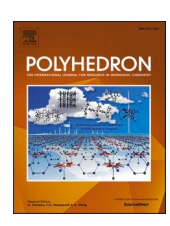


Contents lists available at ScienceDirect

Polyhedron

journal homepage: www.elsevier.com/locate/poly





Vanadacyclobuta-(2,3)-diene rearrangement into a vanadium imido monoazabutadieneallenyl complex

John B. Russell, Sarah M. Smith, Michael R. Gau, Daniel J. Mindiola

Department of Chemistry, University of Pennsylvania, Philadelphia, PA 19104, USA

ARTICLE INFO

Keywords: Metathesis Metallacycle Polymerization Alkylidene

ABSTRACT

We show in this study how the catalyst for the cyclic polymerization of phenylacetylene, a high-spin vanadium (III) complex supported by the β -diketiminate (BDI) scaffold, [(BDI)V(κ^2 -C,C-Me_3SiC_3SiMe_3)] (1) (BDI = [ArNC (CH_3)]_2, Ar = 2,6- iPr_2C_6H_3), can convert thermally or with a Lewis base to a low-spin [V^III] complex [{ArNC (CH_3)CHC(CH_3)C(SiMe_3)}V=NAr] (2). Complex 2 was characterized spectroscopically by multinuclear NMR (1H , ^{13}C , ^{29}Si , ^{51}V), IR, and UV–Vis in addition to single crystal X-ray diffraction analysis. Complex 2 was found to be inactive towards the polymerization of phenylacetylene, unlike its predecessor 1, therefore suggesting that such rearrangement might be the modus operandi for catalyst deactivation. We propose the 1 \rightarrow 2 transformation to involve a denticity change from κ^2 -C,C-Me_3SiC_3SiMe_3 to a κ^1 -alkylidene-alkylnyl, followed by an intra-molecular cross-metathesis pathway involving the V=C bond of the alkylidene-alkynyl ligand with the imine group of the BDI ligand to eventually form the vanadium imido ligand and monoazabutadieneallenyl (MADA $^-$) moiety.

1. Introduction

The past decade has seen a bloom in the field of cyclic polymers due to their inherently unique properties when compared to macromolecules having end groups [1]. In the context of conjugated polymers, initial reports by the Veige group has utilized Mo and W tethered alkylidenes and alkylidynes to synthesize a variety of polymers with cyclic topologies [2–16]. Likewise, the Maeda group has investigated the formation of chiral cyclic conjugated polymers from a variety of low-valent (or masked low-valent) early transition metal complexes with tolanes [17–19]. More recently, our group has shown that cyclic polyphyenylacetylene can be prepared using 3d metal catalysts, with either vanadium alkylidynes [20], or more conveniently, metallacyclobuta-(2,3)-diene (MCB-(2,3)-D) complexes of titanium and vanadium [21]. The latter scaffolds however, are more readily accessible by salt metathesis as described previously Reiß and Beweries [22,23], and thus circumvent the need to prepare the alkylidyne, metallacyclobutadiene, and the deprotiometallacyclobutadiene scaffold. Although MCB-(2,3)-D based complexes of titanium and vanadium can be readily prepared in multigram scales in two steps from MCl₃(THF)₃ (M = Ti, V), Li(BDI) [24], and the dilithio salt [25] of [Me₃SiC₃SiMe₃]²⁻, these systems [21] are limited in their performance ($TOF = 302 \text{ g mol}^{-1}\text{h}^{-1}$) compared to the state of the art tungsten η^2 -alkyne complex $[{}^tBuOCO]W[\eta^2\text{-}(H)CC\ ({}^tBu)]\ [2]\ ({}^tBuOCO^{3-}=\mathit{ipso}\text{-}C_6H_3[2,6\text{-}(C_6H_3\text{-}o\text{-}^tBu)_2])\ (TOF=9.00\times10^6\ g\ mol\text{-}^1h\text{-}^1)$ for the cyclic polymerization of phenylacetylene. The present study reveals how the vanadium catalyst, $[(BDI)V(\kappa^2\text{-}C,C\text{-}Me_3SiC_3SiMe_3)]\ [21]\ (1)\ (BDI=[ArNC(CH_3)]_2,\ and\ Ar=2,6\text{-}^iPr_2C_6H_3),\ undergoes\ a\ rearrangement\ to\ deactivate\ such\ species\ and\ we\ provide\ spectroscopic\ and\ structural\ information\ for\ such\ product\ as\ well\ as\ propose\ a\ likely\ mechanism\ to\ its\ formation.$

Three decades ago, Mortreux and coworkers proposed a mechanism for the formation of polyalkynes using the alkylidyne (tBuO)₃W \equiv C tBu and terminal alkynes (Scheme 1, top). Since an intractable polymer was formed, it was surmised that cycloaddition of the terminal alkyne across the W \equiv C bond followed by deprotonation of the β -carbon in the metallacyclobutadiene (MCBD) scaffold resulted in the formation of a deprotiometallacyclobutadiene (dMCBD). dMCBD then underwent rearrangement to a metal alkylidene-alkynyl in what could be described as a retrocycloaddition step (Scheme 1, top) [26]. Such species was proposed to initiate the propagation step through subsequent alkyne [2+2] cycloaddition steps across the W \equiv C bond, although the topology of the polymer formed was not described.

The isolation of MCBD and dMCBD complexes were originally reported by Schrock [27–30] followed by Weiss [31], Fürstner [32], and

* Corresponding author.

E-mail address: mindiola@sas.upenn.edu (D.J. Mindiola).

Proposed Alkylidene-Alkynyl Species (Mortreux, 1993)

Isolated Alkylidene-Alkynyl Oxo Complex (Mindiola, 2024)

Scheme 1. Top: Proposed reaction involving terminal alkynes with W alkylidyne to form MCBD, followed by a dMCBD, and then to a transient alkylidene-alkynyl. Subsequent cycloadditions of the terminal alkyne and propagation with the alkylidene-alkynyl are also shown. Bottom: Addition of N_2O to a $V^{\rm III}$ MCB-(2,3)-D, which is likely in equilibrium with a alkylidene-alkynyl, to form the $V^{\rm V}$ alkylidene-alkynyl species having a terminal oxo ligand.

Tamm [33,34]. In a previous study by us, it was found that the $V^{\rm III}$ complex 1 could be converted with N₂O to an alkylidene-alkynyl complex [(BDI)V(=O){ κ^1 -C-(=C(SiMe₃)CC(SiMe₃))}] [21] having both terminal alkylidene and oxo ligands (Scheme 1, bottom). We proposed that the MCB-(2,3)-D in 1 would rearrange to the transient alkylidene-alkynyl complex which was then trapped with N₂O to form and oxo and alkylidene-alkynyl ligands.

With the advent of unsaturated scaffolds such as a dMCBD or MCB-(2,3)-D forming an alkylidene-alkynyl ligand, we decided to investigate the reactivity of the former with the vanadium complex 1. Since complex 1 is in fact a catalyst for the cyclic polymerization of phenylacetylene, we probed if this complex could be undergoing a rearrangement during the catalysis which could be rendering it inactive. This could explain why complex 1 exhibited lower activity when compared to the Veige and Maeda's catalysts [2–12,14–19]. Accordingly, we sought different strategies to trap the transient alkylidene-alkynyl species through thermolysis or via a Lewis base using complex 1.

Prior studies by our group have established that 3d metal alkylidenes (Ti and V) [35–39] as well as alkylidynes (V) [40] supported by the BDI ligand can undergo an intramolecular [2+2] cross metathesis between the M—C multiple bond and the imine residue of the BDI supporting ligand according to the two reactions shown in Scheme 2. The process is accelerated when the alkylidene ligand is reduced in sterics at the α -C (e. g, t Bu to t Pr) or inhibited if the BDI ligand was made more sterically encumbering by using β -substituted t Bu groups in the NCCCN ligand backbone [39].

2. Experimental section

2.1. General procedures

All operations were performed in a Labmaster 130 glove box or using standard Schlenk techniques under a nitrogen atmosphere unless otherwise stated. Pentane (Fisher Scientific), was purchased from commercial vendors, thoroughly bubbled with argon, and made anhydrous by passage through columns of activated alumina in a Grubbs-type

Scheme 2. Previous reactivity involving the rearrangement of a titanium neopentylidene and vanadium neopentylidyne and with the imine residue of the BDI supporting ligand (Ar $=2.6^{\rm i} Pr_2 C_6 H_3$). RDS stands for the rate determining step of the reaction.

solvent system. All anhydrous solvents were stored over sodium metal and 4 Å molecular sieves. Benzene–d₆ (C₆D₆) (Cambridge Isotope Laboratories) was dried over a potassium mirror, vacuum transferred to a flame-dried flask and degassed by freeze-pump-thaw cycles prior to use. Celite and 4 Å molecular sieves were activated under vacuum overnight at 200 °C. [(BDI)V(κ²-C,C-Me₃SiC₃SiMe₃)] (1) was prepared according to published procedures [21] (BDI = [ArNC(CH₃)]₂CH⁻, Ar = 2,6-ⁱPr₂C₆H₃). Phenylacetylene (PhC≡CH, Sigma-Aldrich, 98 %) was distilled from magnesium sulfate, degassed by freeze-pump-thaw cycles, and filtered through a column of basic alumina immediately prior to use. 4-dimethylaminopyridine (DMAP, Sigma-Aldrich) was used as received. The crystallographic study was carried out on a single crystal, which was coated with paratone oil, mounted at the end of a cryoloop, and placed in the nitrogen cold stream at 100 K. Data was collected using a Rigaku XtaLAB Synergy-S diffractometers (Mo K_o radiation), operated through the manufacturer's software. The crystal structure was solved using SHELXT (intrinsic phasing) and refined using SHELXL-2018 (least squares) [41,42] typically with data processing carried out in Olex2. NMR spectroscopic studies were recorded on a Bruker Cryo500, UNI500, or AVIII 500 MHz spectrometers. ¹H and ¹³C NMR spectral chemical shifts are referenced to the internal proton or carbon resonances of C₆D₆ (δ 7.16 and δ 128.06). ⁵¹V NMR spectral chemical shifts were referenced to VOCl₃ in C₆D₆ as an external standard (δ 0) and the ²⁹Si NMR spectral chemical shifts were referenced to tetramethylsilane (TMS, δ 0) as an external standard. FT-IR spectroscopic studies were measured on a JASCO FT/IR-4600 spectrometer with samples mounted between KBr windows using the JASCO tablet master device. The sample chamber was flushed with Argon gas to prevent decomposition during measurements. UV-Vis spectroscopic data were obtained on a Cary 5000 UV-Vis-NIR spectrophotometer (Agilent Technologies) using 1 cm quartz cell sealed with a J-Young valve.

2.2. Synthesis of compounds

2.2.1. Thermolysis of [(BDI)V(κ^2 -C,C-Me₃SiC₃SiMe₃)] (1) into [{ArNC (CH₃)CHC(CH₃)C(Si(CH₃)₃)CC(Si(CH₃)₃)}V=NAr] (2)

[(BDI)V(κ^2 -C,C-Me₃SiC₃SiMe₃)] (1) (101.6 mg, 156 μmol, 1.0 equiv) was dissolved in ca. 1 ml of benzene- d_6 (C₆D₆) and the solution was heated to 70 °C for 48 h in which a resulting color change from redorange to dark green was observed. The dark green solution was dried under vacuum and the solution was dissolved in ca. 1 ml of pentane. The concentrated solution was cooled to –35 °C overnight resulting in the formation of green crystals identified as [{ArNC(CH₃)CHC(CH₃)C(Si

(CH₃)₃)CC(Si(CH₃)₃)}V=NAr] (2). The mother liquor was pipetted off, and the crystals dried in vacuo prior to use. Yield: 88.8 mg, 136 μ mol, 87.4 % based on 1. Crystals suitable for X-ray crystallography were separated from a chilled (–35 °C), concentrated pentane solution of 1.

2.2.2. Addition of 4-dimethylaminopyridine (DMAP) to $[(BDI)V(\kappa^2-C,C-Me_3SiC_3SiMe_3)]$ (1) to form $[\{ArNC(CH_3)CHC(CH_3)C(Si(CH_3)_3)CC(Si(CH_3)_3)\}V=NAr\}$ (2)

[(BDI)V(κ²-C,C-Me₃SiC₃SiMe₃)] (1) (50.0 mg, 77 μmol, 1.0 equiv) was dissolved in ca. 0.5 ml of benzene- d_6 (C_6D_6) and the solution was added a ca. 0.5 ml solution of 4-dimethylaminopyridine (DMAP) (9.4 mg, 77 μmol, 1.0 equiv) of benzene- d_6 (C_6D_6), which a resulted in an immediate color change from red-orange to dark green. The dark green solution was dried under vacuum and the solution was dissolved in ca. 1 ml of pentane. The concentrated solution was cooled to –35 °C overnight resulting in the formation of green crystals identified as [{ArNC(CH₃) CHC(CH₃)C(Si(CH₃)₃)}V=NAr] (2). The mother liquor was pipetted off, and the crystals dried in vacuo prior to use. Yield: 38.0 mg, 59 μmol, 76.4 % based on 1. Crystals suitable for X-ray crystallography were separated from a chilled (–35 °C), concentrated pentane solution of 1.

2.2.3. Characterization of $[\{ArNC(CH_3)CHC(CH_3)C(Si(CH_3)_3)CC(Si(CH_3)_3)\}V=NAr]$ (2)

¹H NMR (500 MHz, C_6D_6 , 300 K): δ 7.05–7.17 (m, 3H, C_6H_3 , H_a), 6.78-6.90 (m, 3H, C₆H₃, H_a), 4.38 (septet, 2H, CH(CH₃)₂, H_b), 3.50 (septet, 2H, CH(CH₃)₂, H_c), 3.00 (s, 1H, ArNC(CH₃)C(H)C(CH₃)C(Si (CH₃)₃)CC(Si(CH₃)₃), H_d), 2.64 (s, 3H, ArNC(CH₃)C(H)C(CH₃)C(Si (CH₃)₃)CC(Si(CH₃)₃, Si(CH₃)₃), H_e), 1.42 (dd, 12H, CH(CH₃), H_f), 1.21 (dd, 12H, CH(CH₃), H₂), 1.19 (s, 3H, ArNC(CH₃)C(H)C(CH₃)C(Si(CH₃)₃) CC(Si(CH₃)₃), H_h), 0.37 (s, 9H, (ArNC(CH₃)CHC(CH₃)C(Si(CH₃)₃)CC(Si (CH₃)₃), H_i), 0.06 (s, 9H, (ArNC(CH₃)CHC(CH₃)C(Si(CH₃)₃)CC(Si (CH₃)₃), H_i). ¹³C NMR (126 MHz, C₆D₆, 300 K): δ 125.42 (s, C₆H₃), 124.55 (s, C_6H_3), 124.46 (s, C_6H_3), 123.77 (s, C_6H_3), 122.36 (s, C_6H_3), 106.95 (s, ArNC(CH₃)CHC(CH₃)C(Si(CH₃)₃)CC(Si(CH₃)₃)), 100.77 (s, ArNC(CH₃)CHC(CH₃)C(Si(CH₃)₃)CC(Si(CH₃)₃)), 28.76 (s, CH(CH₃)₂), 27.08 (s, CH(CH₃)₂), 25.77 (s, CH(CH₃)₂), 24.87 (s, CH(CH₃)₂), 24.44 (s, C(H)[C(Me)]₂), 23.14 (s, CH(CH₃)₂), 2.20 (s, Si(CH₃)₃), 1.99 (s, Si (CH₃)₃). 29 Si NMR (99 MHz, C₆D₆, 300 K): δ -0.61, -9.79. 51 V NMR (132 MHz, $C_6D_6,\,300$ K): δ -132.11 ($\nu_{1/2}=462$ Hz). IR, solid, ν (cm $^{-1}$): 1598 cm⁻¹: ν (C=C = C, out of phase), 1386 cm⁻¹: ν (C=C = C, in of phase). UV/Vis, pentane, λ [nm, ε (max/sh, M⁻¹ cm⁻¹)]: 586 (max, 1803), 479 (sh. 2429), 339 (max, 11266), 245 (max, 34792), 221 (max, 34946).

3. Results and discussion

Upon heating a benzene- d_6 solution of 1 for 48 h at 70 °C or by adding DMAP (1 equiv) at room temperature (15 min), a color change from red-orange to green was observed. The green-colored solution was dried *in vacuo*, taken up in *n*-pentane, filtered, and the filtrate concentrated, and cooled to -35 °C to yield green crystals of the vanadium imido having supported by a monoazabutadieneallenyl ligand (MADA⁻), [{ArNC(CH₃)CHC(CH₃)C(Si(CH₃)₃)CC(Si(CH₃)₃)}V=NAr] (2) (Fig. 1, top), based on a combination of structural and NMR spectroscopic studies.

The reaction is essentially quantitative via the thermolytic reaction (87.4 %, isolated yield). Complex **2** could also be formed using DMAP at room temperature (15 min) in comparable yields (76.4 % isolated yield). X-ray quality green crystals of **2** can be obtained from a concentrated pentane solution stored at $-35\,^{\circ}\mathrm{C}$ for 24 h, and a single crystal X-ray diffraction study (sc-XRD) confirmed its assignment as a mononuclear vanadium imido, supported by a chelating MADA $^{-}$ ligand (Fig. 1, bottom). The nomenclature of the MADA $^{-}$ ligand derives from the monoazabutadiene (MAD) ligand described by Tomson, Arnold, and Bergman [43], but also an allenyl (A $^{-}$) moiety thus leading to such a description

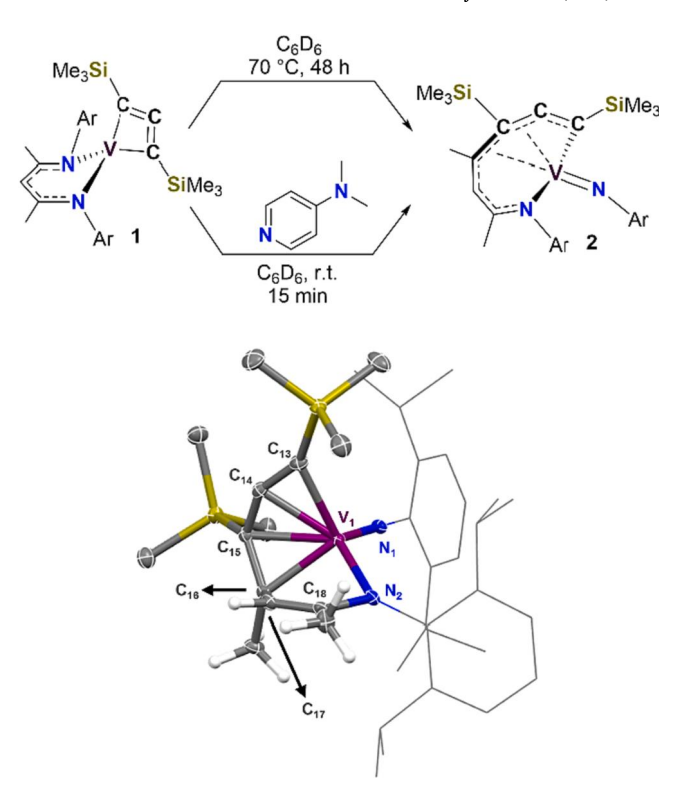


Fig. 1. Top: Synthesis of complex **2** (Ar = 2,6- i Pr₂C₆H₃) from thermolysis or via DMAP addition to **1**. Bottom: sc-XRD of **2** with ellipsoids shown at the 50 % probability level (except for the aryl fragments shown in a wireframe). H-atoms (except on the MADA $^{-}$ ligand backbone) have been omitted for clarity.

of this ligand.

Key structural features of complex 2 are highlighted on the bottom of Fig. 1. The reduction of the V₁-N₁ bond lengths from 1.9751(17) or 1.9814(17) Å in 1 (Fig. 2, left) to 1.679(1) Å in 2 (Fig. 2, right) implies the formation of a vanadium imido, which compares well to previously characterized vanadium imido complexes on rearranged BDI scaffolds shown in Scheme 2, namely the complex [([Ar]NC(CH₃)CHC(CH₃) $CH^{t}Bu)V=NAr(I)$ [36] (1.678(8)Å) and [(${}^{t}BuCC(CH_{3})CHC(CH_{3})N[Ar]$) V=NAr(OTf) [40] (1.671(1)Å) (Ar = 2,6- ${}^{i}Pr_{2}C_{6}H_{3}$). The most notable feature in complex 2 however, is the formation of a chelating MADAligand {ArNC(CH₃)CHC(CH₃)C(Si(CH₃)₃)CC(Si(CH₃)₃)} as the result of the allene fragment undergoing an intramolecular cross-metathesis with the imine residue of the BDI ligand. The monoazabutadiene (MAD, ArNC (CH₃)CHC(CH₃)) residue of the ligand compares well with complexes with similar rearranged BDI scaffolds [35-38]. Specifically, the structure of **2** contains alternating short C₁₇-C₁₈ 1.362(2) Å and long C₁₆-C₁₇ 1.496(2) Å distances (Fig. 2, right), which are characteristic of an asymmetric complex containing a rearranged β-diketiminate ligand

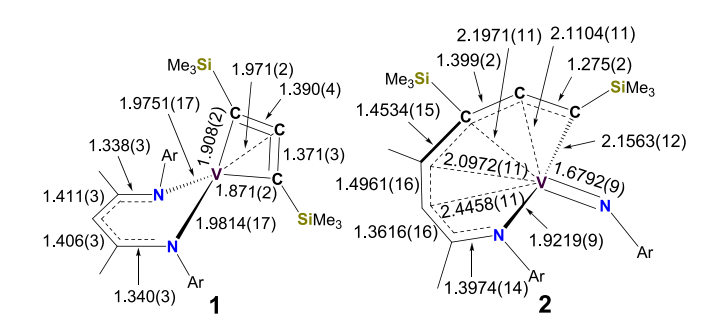
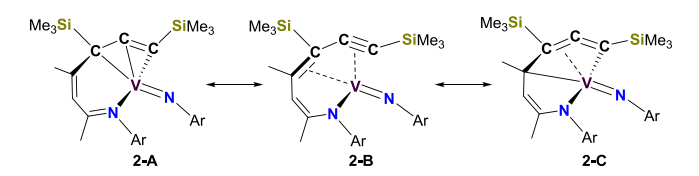


Fig. 2. Comparison of salient metrical parameters between complex 1 (left) and 2 (right). Distances are reported in Å.

[35]. In addition, the C_{18} - N_2 bond length is elongated (1.397(1) Å) compared to the C₁₈-N₂ (1.340(2) Å) and C₁₆-N₁ (1.337(2) Å) bond lengths in 1 (Fig. 2, left), implying the nitrogen atom of the MADAligand in 2 (Fig. 2, right) being more in accord as a neutral donor to the formally $[V^{\rm III}]$ ion. The allenyl moiety (-C(Si(CH_3)_3)CC(Si(CH_3)_3), A^-) of the chelating ligand is oriented nearly perpendicular to the MAD fragment where the plane of the MAD and A⁻ fragments intersect at an angle of 62.81°. The A⁻ fragment exhibits substantially different metrical parameters in comparison with the κ^2 -allene fragment in 1 most likely the result of the larger ring. In 1, the allene's two carbon double bond lengths are quite similar at 1.371(3) and 1.390(4) Å (Fig. 2, left) whereas in 2 the bond distances are 1.399(2) and 1.275(2) Å (Fig. 2, right). In fact, metrical parameters of the A⁻ fragment of **2** are remarkably similar to the vanadium alkylidene-alkynyl complex $\lceil (BDI)V(=O) \rceil \kappa^1 - C - (=C)$ (SiMe₃)CC(SiMe₃))}] [21] bond distances of 1.388(9) and 1.222(2) Å. Thus, one might propose the A⁻ moiety in complex 2 to possess some resonance in accord with an alkynyl ligand (-C-C≡C-) in addition to a bent allenyl (-C=C=C-). However, the bond angle of the fragment in question $\angle C_{13}$ - C_{14} - C_{15} (148.7(1)°) deviates significantly from linearity thus being more consistent with the bent allene fragment in 1 (131.9 (2)°) [21]. The MADA⁻ fragment can therefore adopt several different possible resonance forms with delocalization being dispersed about the 8-membered ring (Scheme 3). For simplicity we do not show other possible resonances where the ligand and the vanadium center have radical character and could weakly couple. Based on the metrical parameters we propose V-C interactions to take place with the A⁻ motif as well as with the λ -C of the ring. Whereas resonance **2-A** implies a trianionic charge localized about the allenyl motif in accordance with a VV ion, resonance 2-B suggests somewhat of a lesser extent of backbonding with the alkynyl and alkene motifs with a low-spin V^{III} ion. Resonance 2-C on the other hand suggests a slightly more distributed set of charges around the 8-membered ring. We propose contributions from all possible resonances based on the metrical parameters observed in the sc-XRD study of 2.

Complex 2 is a diamagnetic, consistent with a low-spin VIII or possibly a V^V ion, thus we relied on multinuclear NMR spectroscopy to further characterize this species. The ¹H NMR spectrum of 1 (Fig. S1) spectrum clearly shows the formation of a single diamagnetic species in solution. A singlet at δ 3.00 (Fig. S1, H_d) was determined to be the methine hydrogen on the backbone of the MAD motif. Complex 2 also shows two septets at δ 4.38 (Fig. S1, H_b) and 3.50 (Fig. S1, H_c) for the isopropyl methines as well as two singlets at δ 2.65 (Fig. S1, H_e) and 1.19 (Fig. S1, H_b) for the former β-methyl groups on the BDI backbone in 1. Two intense resonances at δ 0.37 (Fig. S1, H_i) and 0.06 (Fig. S1, H_i) were assigned as the two inequivalent trimethylsilyl groups. To unambiguously elucidate the structure of 2 we relied on multidimensional and heteronuclear NMR spectroscopic studies. A combination of a ¹H–¹H COSYand H-13C HSQC NMR spectroscopic experiments (Fig. 3, top) highlights key correlations in 2. Specifically, the methine resonance on the MADA⁻ ligand at δ 3.00 correlating to a resonance at δ 106.56 in the carbon NMR trace for the γ -C of MAD motif. The latter experiment also allowed for assignment of other groups such as the trimethylsilyl, methyl, diisopropyl, and aryl fragments in 2 (Fig. S6-S8). To further assign the remaining carbon resonances in 2 we employed a ¹H-¹³C HMBC NMR spectroscopic experiment (Fig. S9). Resonances for the remaining carbons on the MAD residue were found at δ 148.3 and 155.7 and correlated with the hydrogens on the methyl groups on the ligand



Scheme 3. Proposed resonances for the metallaaza-diene-yne scaffold in 2.

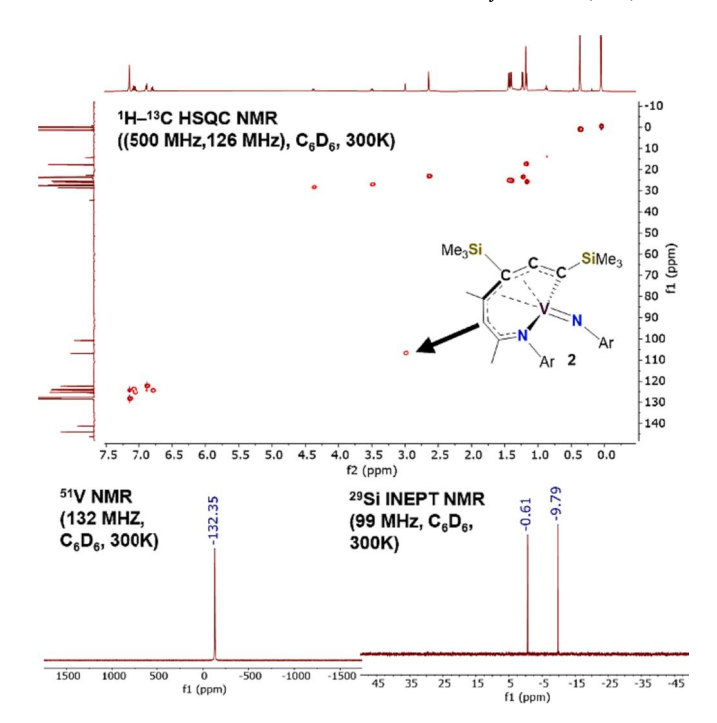


Fig. 3. Top: $^{1}H_{-}^{13}C$ HSQC NMR((500 MHz, 126 MHz), $C_{6}D_{6}$, 300 K) spectrum of **2**, with the inset showing the assignment of the methine peak at (^{1}H : 3.00 ppm, ^{13}C : 106.56 ppm). Bottom Left: ^{51}V NMR (132 MHz, $C_{6}D_{6}$, 300 K) spectrum of **2**. Bottom Right: ^{29}Si NMR (99 MHz, $C_{6}D_{6}$, 300 K) spectrum of **2**.

(Fig. S10). Aryl carbon atoms and trimethylsilyl groups were also assigned based on similar correlations to nearby C—H groups (Fig. S12). The observation of this downfield carbon resonance in the 13 C NMR at δ 100.31 provides credence to the MADA- ligand having an allenyl (-C=C=C-M) moiety rather than a pendant alkyne (-C-C≡C-). Unfortunately, the other two carbon resonances on the allenyl fragment (-C=C=C-M) were not located. A possible explanation for the low intensity in these carbons might be due to the lack of protons directly bonded to each which in turn increases the relaxation time for those carbons. In addition, the carbons of interest are near the quadrupolar ⁵¹V nuclei (⁵¹V, 99.75 % abundance, $I = \frac{7}{2}$), which in turn render these resonances quite broad [44]. The ⁵¹V NMR spectrum (Fig. 3, bottom left) of complex **2** showed one resonance at $\delta - 132.11$ ($\nu_{1/2} = 462$ Hz, Fig. 3, bottom left), which compares quite nicely to the previously characterized complex (^tBuC=C(Me)CHC(Me)N[Ar])V=NAr(OTf) [40] (δ -165.3). Lastly, the ²⁹Si INEPT NMR spectrum (Fig. 3, bottom right) contains two signals at δ -0.61 and -9.79 for the two chemically inequivalent SiMe₃ groups in the MADA⁻ ligand of 2 (Fig. 3, bottom right).

In addition to structural and NMR spectral studies, IR and UV-Vis studies were also carried out for 2. The IR spectra of 2 (Fig. S15) shows diagnostic stretches of C=C=C unit at 1386 cm⁻¹ and 1598 cm⁻¹. This deviates slightly from 1 [21] whose C=C=C out-of-phase stretch is at 1530 cm⁻¹. Reiß and Beweries observed C=C=C out-of-phase stretching frequencies at 1729 cm⁻¹ and at 1731 cm⁻¹ for MCB-(2,3)-D titanium [22] and zirconium [23] complexes, respectively. The UV-Vis spectral data of **2** (Fig. S16) is also quite diagnostic of a V^{III} complex as there are two electronic bands with small molar absorptivity values (ϵ) at 586 nm $(\epsilon=1803\,\text{M}^{-1}\text{cm}^{-1})$ and 479 nm ($\epsilon=2429\,\text{M}^{-1}\text{cm}^{-1}$). These two bands can be attributed to the two d-d transitions for a V^{III} ion. In comparison, the high-spin d^2 precursor **2** exhibits two d-d transitions at 770 nm ($\varepsilon =$ 156 $M^{-1}cm^{-1}$) and 416 ($\varepsilon = 3088 M^{-1}cm^{-1}$) [21]. Other absorptions in 2 can be attributed to charge transfer bands at 339 nm ($\varepsilon = 11266$ $M^{-1}cm^{-1}$), 245 nm ($\epsilon = 34792~M^{-1}cm^{-1}$), and 221 nm ($\epsilon = 34946$ $M^{-1}cm^{-1}$).

We propose complex ${\bf 2}$ to form akin to how titanium and vanadium

alkylidene complexes rearrange with the BDI ligand (vide supra, Scheme 1). Upon thermolysis or via addition of a Lewis base, the MCB-(2,3)-D scaffold in 1 undergoes a denticity change from κ^2 to κ^1 via the formation of a vanadium alkylidene (bottom of Scheme 1). The V=C bond then undergoes an intramolecular cross-metathesis with the imine fragment of the BDI ligand to form a vanadium imido and the chelating MADA⁻ ligand {ArNC(CH₃)CHC(CH₃)C(Si(CH₃)₃)}-.

Complex 2 was investigated as a potential precatalyst for the formation of polyphenylacetylene from phenylacetylene. However, after several trials at different concentrations of monomer or metal complex, as well as varying solvents it was determined that 2 was not catalytically competent. The inactivity of 2 towards the polymerization of phenylacetylene suggests tantalizingly that this rearrangement could be one plausible deactivating mode of catalyst 1.

4. Conclusion

In conclusion we reported the rearrangement of a cyclic conjugated polymer catalyst 1 into a catalytically inactive vanadium imido complex 2 containing an unusual ligand scaffold, a monoazabutadieneallenyl ligand which we abbreviate as MADA⁻. The deactivation of the cyclic polyphenylacetylene catalyst 1 is proposed to occur via an intramolecular cross-metathesis rearrangement involving a transient vanadium alkylidene with the imine moiety of the BDI ligand. Having found this likely mode of deactivation, we are now exploring more robust chelating scaffolds of Ti and V with the MCB-(2,3)-D ligand which lack vulnerable sites for cross-metathesis with a transient alkylidene-alkynyl ligand.

CRediT authorship contribution statement

John B. Russell: Writing – review & editing, Writing – original draft, Methodology, Investigation, Formal analysis. Sarah M. Smith: Investigation. Michael R. Gau: Investigation, Formal analysis. Daniel J. Mindiola: Writing – review & editing, Supervision, Funding acquisition.

Declaration of competing interest

The authors declare the following financial interests/personal relationships which may be considered as potential competing interests: J. B.R and D.J.M have filed a U.S. Provisional Application No. 63/488,610, March 6, 2023.

Data availability

Data will be made available on request.

Acknowledgments

We thank the University of Pennsylvania and the U.S. National Science Foundation (NSF; CHE-2154620 to D.J.M.). The Research Experience for Undergraduates program, NSF CHE-1851640, is also thanked for funding of S.M.S. J.B.R. thanks the Vagelos Institute for Energy Science and Technology (VIEST) for a predoctoral fellowship. The authors would also like to thank Dr. Jun Gu for invaluable help in the NMR spectral analysis. We dedicate this work to Professor Peter T. Wolczanski, a giant in the synthesis, reactivity, and mechanistic studies of low-coordinate metal fragments of early- and mid-transition metals. Happy 70th birthday Pete!

Appendix A. Supplementary data

Supplementary data to this article can be found online at https://doi.org/10.1016/j.poly.2024.116913.

References

- [1] F.M. Haque, S.M. Grayson, Nat. Chem. 12 (2020) 433-444.
- [2] C.D. Roland, H. Li, K.A. Abboud, K.B. Wagener, A.S. Veige, Nat. Chem. 8 (2016) 791–796.
- [3] S.A. Gonsales, T. Kubo, M.K. Flint, K.A. Abboud, B.S. Sumerlin, A.S. Veige, J. Am. Chem. Soc. 138 (2016) 4996–4999.
- [4] S.S. Nadif, T. Kubo, S.A. Gonsales, S. VenkatRamani, I. Ghiviriga, B.S. Sumerlin, A. S. Veige, J. Am. Chem. Soc. 138 (2016) 6408–6411.
- [5] W. Niu, S.A. Gonsales, T. Kubo, K.C. Bentz, D. Pal, D.A. Savin, B.S. Sumerlin, A. S. Veige, Chemistry 5 (2019) 237–244.
- [6] C.D. Roland, S. VenkatRamani, V.K. Jakhar, I. Ghiviriga, K.A. Abboud, A.S. Veige, Organometallics 37 (2018) 4500–4505.
- [7] Z. Miao, T. Kubo, D. Pal, B.S. Sumerlin, A.S. Veige, Macromolecules 52 (2019) 6260–6265.
- [8] Z. Miao, D. Pal, W. Niu, T. Kubo, B.S. Sumerlin, A.S. Veige, Macromolecules 53
- (2020) 7774–7782.

 [9] D. Pal, Z. Miao, J.B. Garrison, A.S. Veige, B.S. Sumerlin, Macromolecules 53 (2020)
- 9717–9724.

 [10] Z. Miao, A.M. Esper, S.S. Nadif, S.A. Gonsales, B.S. Sumerlin, A.S. Veige, React.
- Funct. Polym. 169 (2021) 105088.

 [11] Z. Miao, S.A. Gonsales, C. Ehm, F. Mentink-Vigier, C.R. Bowers, B.S. Sumerlin, A.
- [11] Z. Miao, S.A. Gonsales, C. Ehm, F. Mentink-Vigier, C.R. Bowers, B.S. Sumerlin, A. S. Veige, Nat. Chem. 13 (2021) 792–799.
- [12] Z. Miao, D. Konar, B.S. Sumerlin, A.S. Veige, Macromolecules 54 (2021) 7840–7848.
- [13] V.K. Jakhar, Y.-H. Shen, S.-M. Hyun, A.M. Esper, I. Ghiviriga, K.A. Abboud, D. W. Lester, A.S. Veige, Organometallics 42 (2023) 1339–1346.
- [14] V. Jakhar, D. Pal, I. Ghiviriga, K.A. Abboud, D.W. Lester, B.S. Sumerlin, A.S. Veige, J. Am. Chem. Soc. 143 (2021) 1235–1246.
- [15] U. Mandal, I. Ghiviriga, K.A. Abboud, D.W. Lester, A.S. Veige, J. Am. Chem. Soc. 143 (2021) 17276–17283.
- [16] A.M. Beauchamp, J. Chakraborty, I. Ghiviriga, K.A. Abboud, D.W. Lester, A. S. Veige, J. Am. Chem. Soc. 145 (2023) 22796–22802.
- [17] S. Sueyoshi, T. Taniguchi, S. Tanaka, H. Asakawa, T. Nishimura, K. Maeda, J. Am. Chem. Soc. 143 (2021) 16136–16146.
- [18] D. Nakaguchi, T. Taniguchi, T. Nishimura, K. Maeda, Macromolecules 56 (2023) 5873–5880.
- [19] M. Miyairi, T. Taniguchi, T. Nishimura, K. Maeda, Angew. Chem., Int. Ed., 62 (2023), e202302332.
- [20] M.G. Jafari, J.B. Russell, H. Lee, B. Pudasaini, D. Pal, Z. Miao, M.R. Gau, P. J. Carroll, B.S. Sumerlin, A.S. Veige, M.-H. Baik, D.J. Mindiola, J. Am. Chem. Soc. 146 (2024) 2997–3009.
- [21] J.B. Russell, D. Konar, T. Keller, M.R. Gau, P.J. Carroll, J. Telser, D.W. Lester, A. S. Veige, B.S. Sumerlin, D.J. Mindiola, Angew. Chem., Int. Ed. (2024) e202318956.
- [22] F. Reiß, M. Reiß, J. Bresien, A. Spannenberg, H. Jiao, W. Baumann, P. Arndt, T. Beweries, Chem. Sci. 10 (2019) 5319–5325.
- [23] X. Shi, S. Li, M. Reiß, A. Spannenberg, T. Holtrichter-Rößmann, F. Reiß, T. Beweries, Chem. Sci. 12 (2021) 16074–16084.
- [24] P.H.M. Budzelaar, A.B. van Oort, A.G. Orpen, Eur. J. Inorg. Chem. 1998 (1998) 1485–1494.
- [25] F. Reiß, M. Reiß, A. Spannenberg, H. Jiao, W. Baumann, P. Arndt, U. Rosenthal, T. Beweries, Chem. Eur. J. 24 (2018) 5667–5674.
- [26] A. Bray, A. Mortreux, F. Petit, M. Petit, T. Szymanska-Buzar, J. Chem. Soc., Chem. Commun. (1993) 197–199.
- [27] L.G. McCullough, M.L. Listemann, R.R. Schrock, M.R. Churchill, J.W. Ziller, J. Am. Chem. Soc. 105 (1983) 6729–6730.
- [28] L.G. McCullough, R.R. Schrock, J.C. Dewan, J.C. Murdzek, J. Am. Chem. Soc. 107 (1985) 5987–5998.
- [29] R.R. Schrock, J.H. Freudenberger, M.L. Listemann, L.G. McCullough, J. Mol. Catal. 28 (1985) 1–8.
- [30] H. Strutz, J.C. Dewan, R.R. Schrock, J. Am. Chem. Soc. 107 (1985) 5999–6005.
- [31] K. Weiss, R. Goller, G. Loessel, J. Mol. Catal. 46 (1988) 267–275.
- [32] J. Heppekausen, R. Stade, A. Kondoh, G. Seidel, R. Goddard, A. Fürstner, Chem. Eur. J. 18 (2012) 10281–10299.
- [33] B. Haberlag, M. Freytag, C.G. Daniliuc, P.G. Jones, M. Tamm, Angew. Chem., Int. Ed. 51 (2012) 13019–13022.
- [34] H. Ehrhorn, D. Bockfeld, M. Freytag, T. Bannenberg, C.E. Kefalidis, L. Maron, M. Tamm, Organometallics 38 (2019) 1627–1639.
- [35] F. Basuli, B.C. Bailey, J. Tomaszewski, J.C. Huffman, D.J. Mindiola, J. Am. Chem. Soc. 125 (2003) 6052–6053.
- [36] F. Basuli, U.J. Kilgore, X. Hu, K. Meyer, M. Pink, J.C. Huffman, D.J. Mindiola, Angew. Chem. Int. Ed. Engl. 43 (2004) 3156–3159.
- [37] F. Basuli, B.C. Bailey, J.C. Huffman, D.J. Mindiola, Organometallics 24 (2005) 3321–3334.
- [38] F. Basuli, B.C. Bailey, L.A. Watson, J. Tomaszewski, J.C. Huffman, D.J. Mindiola, Organometallics 24 (2005) 1886–1906.
- [39] B.C. Bailey, F. Basuli, J.C. Huffman, D.J. Mindiola, Organometallics 25 (2006) 3963–3968.
- [40] F. Basuli, B.C. Bailey, D. Brown, J. Tomaszewski, J.C. Huffman, M.-H. Baik, D. J. Mindiola, J. Am. Chem. Soc. 126 (2004) 10506–10507.
- [41] G.M. Sheldrick, Acta Crystallogr. A 64 (2008) 112–122.
- [42] G.M. Sheldrick, Acta Crystallographica Section a: Foundations and Advances 71 (2015) 3–8.
- [43] N.C. Tomson, J. Arnold, R.G. Bergman, Organometallics 29 (2010) 5010-5025.
- [44] A. Brisdon, in: Fluorine Chemistry, 2023. https://fluorine.ch.man.ac.uk/ (accessed November 10th, 2023).